Measurement of $C^+ + e^- + e^-$ and $CO^+ + e^-$ Recombination in Carbon Monoxide Flows

MICHAEL G. DUNN*
Cornell Aeronautical Laboratory Inc., Buffalo, N. Y.

The three-body recombination rate coefficient for the reaction $C^+ + e^- + e^- \underset{k_{r_1}}{\rightarrow} C + e^-$ has been measured in the inviscid nozzle flow of a reflected-shock tunnel and found to be given by $k_{r_1} = (6.0 \pm 2) \times 10^{-8}\ T_e^{-4.5}$ cm^6/sec for the electron temperature range of approximately 1500° to 7000°K. For this particular reservoir condition, the three-body C^+ deionization reaction was the only one of importance in the expansion. In addition, the dissociate-recombination rate coefficient for the reaction $CO^+ + e^- \underset{k_{r_2}}{\rightarrow} C + O$ was also measured and found to be given by $k_{r_2} = (2.5 \pm 0.5) \times 10^{-2}\ T_e^{-1.5}$ cm^3/sec for the electron temperature range of approximately 1200°–6300°K. At this reservoir condition, several of the charge-transfer reactions were found to be important in the nonequilibrium expansion. Since rate coefficients at elevated temperatures are not available for these reactions, it was necessary to estimate values based on other information. The influences of these estimates on the rate coefficient for the deionization of CO^+ are discussed. The measurements discussed here were performed in carbon monoxide that has expanded from equilibrium reservoir conditions of 7060°K at 17.3 atm pressure and from 6260°K at 10.0 atm pressure. The electron density was measured at several area ratios in the expansion using microwave interferometers. The electron temperatures and electron densities on the nozzle centerline were simultaneously measured at these locations using voltage-swept thin-wire Langmuir probes. The measured electron temperatures were used in determining the rate coefficients from the number-density data.

Introduction

THE next step in space exploration beyond the moon project is most likely the exploration of the planets Mars and Venus. One of the basic objectives of the first missions will probably be the determination of the composition of the atmosphere, not only near the surface, but throughout the entry trajectory. The success of these missions is partially dependent upon the ability to calculate the gas composition in the plasma surrounding the entry body. At the present time, reaction rate coefficients for several of the reactions of possible importance in the C–O–N system are not well known. This lack of data motivated the studies described here. At the present time attention is confined to reactions involving ions and/or electrons because of the potential communication blackout problem.

Previous measurements reported[1–3] from this laboratory have presented rate coefficient data for the dissociative recombination of NO^+, N_2^+, and O_2^+ which are also of importance in the C–O–N system. The purpose of this paper is to present rate-coefficient data, obtained in the same manner, for the electron depletion reactions

$$C^+ + e^- + e^- \underset{k_{r_1}}{\rightarrow} C + e^- \qquad (1)$$

and

$$CO^+ + e^- \underset{k_{r_2}}{\rightarrow} C + O \qquad (2)$$

For the gasdynamic conditions of these experiments it was anticipated on a theoretical basis that the electron temperature would be different from the heavy-particle translational temperature during some regions of the expansion. The electron temperature was therefore measured and used in the data correlation.

Many authors[4–11] have published theoretical predictions and experimental measurements of the rate coefficient for the class of reactions given by $M^+ + e^- + e^- \rightarrow M + e^-$ where M is an atomic ion. Curry[4] has recently summarized these papers and placed them in their proper perspective thereby making a similar discussion here unnecessary with the exception of brief mention of the theoretical results of Makin and Keck[5] and Mansbach and Keck.[6] The results of these authors are used in this paper for comparison with the current and previous experimental data.

Makin and Keck[5] use a classical phase-space concept in which a point in phase space is used to represent the impact point of the three colliding particles and a distribution of these points is assumed to correspond to a gas in thermodynamic equilibrium. The authors propose a "trial" surface which separates the free and bound states of the electron-ion pair at a selected energy which is less than the dissociation limit. By minimizing the rate at which representative points cross the trial surface, a least upper bound to the recombination rate can be calculated. As will be shown later, this theory does give an upper bound for the helium, hydrogen, and nitrogen data but not for the argon, cesium and mercury data.

More recently, Mansbach and Keck[6] have used Monte Carlo trajectory calculations in conjunction with the variational theory and arrived at a smaller value for the steady state collisional recombination rate coefficient. In this later work, the authors have removed a restriction on the previous study[5] which resulted in neglecting re-excitation in the cascade process.

The only measurement for the three-body recombination relevant to the C–O–N system is that obtained by Park[16] at an electron temperature of 10,000°K for the reaction $N^+ + e^- + e^- \rightarrow N + e^-$. His experiments were performed in the expanding-flow region of an electric-arc plasma wind tunnel. He used the hydrogen-beta line broadening technique to determine the electron density. The electron temperature was

Received April 2, 1971; revision received June 29, 1971. This research was supported by NASA, under Contract NAS 1-9627. The author would like to thank J. Lordi of the Cornell Aeronautical Laboratory for the many fruitful discussions during the course of this work and J. Moselle of Cornell Aeronautical Laboratory for performing the nonequilibrium calculations.

Index categories: Thermochemistry and Chemical Kinetics; Reactive Flows.

* Principal Engineer, Aerodynamic Research Department. Member AIAA.

obtained from the ratio of spectral lines of nitrogen, 5617 Å and 4935 Å. Park[17] also discusses a theoretical technique for calculating the recombination rate coefficients for the deionization of atomic ions. He compares the results of his calculations for N^+ to those of Hinnov and Hirschberg (He^+) and illustrates good agreement. Experimental data for the reaction $CO^+ + e^- \rightarrow C + O$ have been reported by Mentzoni and Donohoe for electron temperatures of approximately 273°K[18] and 775°K[19]. The authors used microwave diagnostics to study the electron decay in the afterglow following a pulsed d.c. discharge in carbon monoxide.

In the present experiments, both the electron temperature and number density were measured. This electron temperature was used in computing the variation of number density along the nozzle. The recombination rate coefficient was then adjusted until the calculated number density agreed with the microwave-interferometer data.

Experimental Apparatus and Technique

A pressure driven shock tube was used to produce a reservoir of high-temperature carbon monoxide which was subsequently expanded in a conical nozzle. The test gas used in these experiments was supplied by Lif-O-Gen, Inc. A chemical analysis of the gas indicated the following: 25 ± 5 ppm of nitrogen, argon less than 2 ppm, carbon dioxide less than 10 ppm, helium less than 4 ppm, hydrogen less than 4 ppm, methane less than 2 ppm, oxygen less than 2 ppm, and water less than 1 ppm.

The electron number densities were measured at 11.5, 21.5, 31.5 and 41.5 in. from the nozzle throat using microwave interferometers operating at frequencies of either 35 or 17 GHz. One inch downstream of each microwave interferometer measuring station, thin-wire Langmuir probes were used on the nozzle centerline to measure the electron temperature and electron density. The microwave interferometers and the experimental procedure are discussed in more detail in Ref. 1.

The probes used in these experiments were constructed by surrounding 0.004 in. diam tungsten wires with a quartz envelope, leaving a nominal 0.400 in. length of bare wire exposed. Immediately prior to each run, the tungsten oxide is removed by placing the probe in a dilute solution of sodium hydroxide and passing approximately 400 μa of current through the circuit for approximately 10 min.

Method of Determining Rate Coefficient

Two reflected-shock reservoir conditions were used to obtain the reaction rate coefficients for the deionization reactions given by Eqs. (1) and (2). At the first condition the test gas was expanded from an equilibrium condition of 7060°K and 17.3 atm pressure and the dominant chemical reaction taking place in the expansion was $C^+ + e^- + e^- \rightarrow C + e^-$. All of the other reactions given in Table 1 were included in the nonequilibrium nozzle-flow calculations performed for this reservoir condition, but perturbation of their rate coefficients did not have a significant influence on the predicted electron-density distribution. At the second condition, 6260°K and 10.0 atm pressure, the reactions involving neutral species only were still unimportant, but several reactions involving charged species were important. By accepting a set of rate coefficients for the charge-transfer reactions it was possible to deduce the rate coefficient for the dissociative recombination reaction $CO^+ + e^- \rightarrow C + O$. In the remainder of the paper, the method of data analysis is described and experimental results are presented for each of the previously mentioned conditions.

Procedure for Calculating Electron-Density Distribution and Chemical Model Utilized

The nonequilibrium nozzle-flow calculations noted previously were performed with the nozzle-flow computer program described in Ref. 20. This program computes the solution for the gasdynamic properties and chemical composition in the expansion of an arbitrary gas mixture from an equilibrium reservoir state through a given nozzle geometry. The vibrational and electronic degrees of freedom of the species are assumed to maintain thermodynamic equilibrium but the chemical reactions are allowed to proceed at finite rates. A more detailed description of the modifications made to the standard version of this program in order to perform the calculations discussed here is given in Ref. 2. In this study the following species were included: CO, O_2, CO_2, C, O, CO^+, O_2^+, C^+, O^+ and e^-. The chemical-kinetics model used in the earlier calculations was significantly larger than the one shown in Table 1, which was obtained by eliminating from the initial model the unimportant reactions. Among these unimportant reactions were the three-body reactions of the type $M^+ + e^- + N \rightarrow M + N$ where N is a heavy particle. The contribution of radiative recombination was also assessed and found to be unimportant for the conditions of interest here.

Reaction rate coefficients for reactions 1–6 were estimated to be represented by the expressions given in Table 1. For the expanding flow situation of interest here, more accurate knowledge of these rate coefficients is not necessary because the neutral species concentrations in the expansion were es-

Table 1 Chemical kinetics model used in data correlation

No.	Reaction	Third body, M	Rate coefficient in direction shown, in cm^3/sec or cm^4/sec	
1	$O_2 + M \xrightarrow{k_f} 2O + M$	O	$3.49 \times 10^{-6}\ T^{-0.5}$	$\exp(-1.1796 \times 10^5/R_oT)$
2	$O_2 + M \xrightarrow{k_f} 2O + M$	C,CO,CO_2	$1.99 \times 10^{-3}\ T^{-1.5}$	$\exp(-1.1796 \times 10^5/R_oT)$
3	$CO + M \xrightarrow{k_f} C + O + M$	C,O,O_2,CO,CO_2	$7.45 \times 10^{-5}\ T^{-1.0}$	$\exp(-2.56 \times 10^5/R_oT)$
4	$CO_2 + M \xrightarrow{k_f} O + CO + M$	C,O,O_2,CO,CO_2	$1.46 \times 10^{-1}\ T^{-2.0}$	$\exp(-1.256 \times 10^5/R_oT)$
5	$CO + CO \xrightarrow{k_f} C + CO_2$		$3.86 \times 10^{-15}\ T^{0.5}$	$\exp(-1.305 \times 10^5/R_oT)$
6	$O + CO \xrightarrow{k_f} C + O_2$		$4.52 \times 10^{-13}\ T^{0.5}$	$\exp(-1.381 \times 10^4/R_oT)$
7	$CO + CO^+ \xrightarrow{k_f} CO_2 + C^+$		$1.77 \times 10^{-1}\ T^{0.5}$	$\exp(-6.705 \times 10^4/R_oT)$
8	$CO + C^+ \xrightarrow{k_f} C + CO^+$		$1.00 \times 10^{-12}\ T^{0.5}$	$\exp(-6.336 \times 10^4/R_oT)$
9	$O + C^+ \xrightarrow{k_f} C + O^+$		$1.11 \times 10^{-11}\ T^{0.5}$	$\exp(-5.416 \times 10^4/R_oT)$
10	$CO + O^+ \xrightarrow{k_f} O + CO^+$		$1.81 \times 10^{-12}\ T^{0.5}$	$\exp(-9.222 \times 10^3/R_oT)$
11	$O + CO^+ \xrightarrow{k_f} O_2 + C^+$		$9.10 \times 10^{-12}\ T^{0.5}$	$\exp(-7.470 \times 10^4/R_oT)$
12	$CO^+ + e^- \xrightarrow{k_r} C + O$		(Determined from these experiments see Fig. 9)	
13	$C^+ + e^- + e^- \xrightarrow{k_r} C + e^-$		(Determined from these experiments see Fig. 6)	
14	$O^+ + e^- + e^- \xrightarrow{k_r} O + e^-$		$5.2 \times 10^{-8}\ T_e^{-4.5}$	

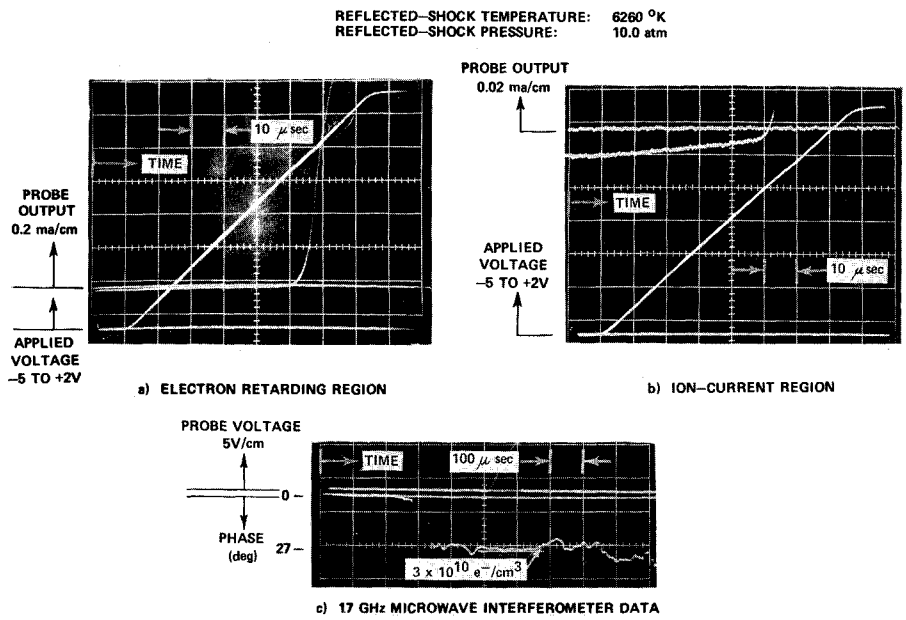

Fig. 1 Typical probe characteristics and microwave-interferometer data in carbon monoxide plasma at 32.5 in from the nozzle throat.

sentially frozen at the nozzle throat (near equilibrium) values and thus the neutral reactions had little influence on the ion concentrations in the expansion. Much more important for these studies was the rate coefficients for the ion-molecule and ion-atom reactions.[7–10] Throughout the expansion these reactions were all proceeding in the direction opposite to that written in Table 1. The only available experimental data for these reactions were those obtained by Fehsenfeld, Schmeltekopf and Ferguson[21] at 300°K for the reaction $CO_2 + C^+ \rightarrow CO + CO^+$. To the author's knowledge, rate coefficients have not been measured for the remaining three reactions. These rates were therefore estimated at 300°K and extrapolated to higher temperatures as described by the equations given in Table 1. Compared to reactions 7–10, reaction 11 was considerably less important.

In all of the nozzle-flow calculations performed in this study, the prescribed nozzle cross-sectional area was that of the inviscid core. The boundary-layer displacement thickness was computed using the method of Burke and Wallace.[22] For the conditions of these experiments the boundary-layer correction is small.

Langmuir-Probe and Microwave-Interferometer Measurements

A typical swept-voltage probe characteristic obtained on the nozzle centerline for a reservoir condition of 7060°K and 17.3 atm is shown in Figs. 1a and 1b. These oscilloscope records were recorded simultaneously using two oscilloscopes with the vertical sensitivities adjusted to emphasize the electron-retarding region, from which the electron temperature was deduced, and the ion-current region, from which the electron density was obtained. The voltage applied to the probe was recorded on the lower channel of each oscilloscope. In these experiments the probe voltage was swept from −5 to +2 volts relative to ground potential. Figure 1c shows the phase-shift of the incident energy and the voltage sweep relative to the test time obtained from a microwave interferometer located 1 in. upstream of the Langmuir probe. The attenuation of the incident microwave energy was also recorded but was found to be less than 0.1 db for this location in the expansion.

The electron density was obtained from the Langmuir-probe data using the free-molecular flow theory of Laframboise.[23] In these calculations, the dominant ion was assumed to be C^+ consistent with the calculated species concentrations presented in Figs. 2a and 2b for the two reservoir conditions. However, in contrast to previous[1–3] results obtained at this laboratory using several different test gases (air, nitrogen, oxygen and argon), the electron densities obtained in these experiments from the Langmuir-probe data were consistently less than the corresponding values obtained from the microwave interferometers by a factor of 1.4–2.0 at the downstream stations.

The cause of this apparent inconsistency between the two diagnostic techniques does not appear to be related to collisional effects which have been shown by Talbot and Chou[24] to produce such a result. The relative magnitudes of the mean free paths $\lambda_{i-\eta}$, $\lambda_{\eta-\eta}$, $\lambda_{e-\eta}$, λ_{i-i}, and λ_{e-e} were calculated using the expressions summarized by Sonin[25] and are presented in Fig. 3 for one of the experimental conditions. With the exception of λ_{i-i}, which is somewhat smaller at this experimental condition, these values are not significantly different from those obtained for the previous nitrogen work of Dunn and Lordi[26] in which the probe and microwave-interferometer results were found to be in good agreement at the downstream stations. Initially it was felt that the smaller value of the ion-ion mean free path was contributing to the disagreement. The second experimental condition was then completed and a quantitatively similar inconsistency between the probe and microwave-interferometer results was still present. However, for this experimental condition, all of the mean free paths were comparable to those for the previous nitrogen work.

The calculated ion-species distributions suggest that the correct ion has been used in the probe data reduction and the calculated mean free paths suggest that the probe results should be free of collisional effects. It is realized that if the collected ion were CO^+ instead of C^+, then the probe and interferometer results would be in relatively good agreement. However, in order for this to be the case, the mobility of the CO^+ ion would necessarily be much larger (see Figs. 2a and 2b for relative concentrations) than that of C^+ and in light of existing information this is an unlikely result.

The anomaly described above is disturbing because the only check one has on proper probe operation is by comparison of the electron-density results with an accepted measurement standard, in our case the microwave interferometer. However, because the probe-deduced electron densities are not essential to the rate-coefficient determination, the problem was not pursued further. The electron temperatures obtained from the probe results are, however, used for the rate-coefficient studies. The measured electron temperatures

have been accepted as correct on the basis of past experience[1-3,26] with Langmuir-probe operation. Later in the text, the influence of the electron temperature on the rate coefficient results will be illustrated.

Determination of Rate Coefficient

It was previously mentioned that the rate coefficient for the deionization of C^+ by the reaction $C^+ + e^- + e^- \rightarrow C + e^-$ and the deionization of CO^+ by the reaction $CO^+ + e^- \rightarrow C + O$ have been measured at two separate reservoir conditions. In this section the measurements obtained at each of the experimental conditions are discussed separately.

$C^+ + e^- + e^-$ Reaction

The electron-temperature measurements performed at this experimental condition are compared in Fig. 4 to the calculated heavy-particle translational temperature. Measurements were made at axial distances from the nozzle throat of 12.5, 22.5, 32.5 and 42.5 in. ($A/A^* = 70{,}230$, 470 and 780). Using the electron energy equation, Lordi and Dunn[27] have previously illustrated that for an expanding nitrogen flow the electron temperature can be expected to be greater than the heavy-particle translational temperature with increasing expansion ratio. Apply the same technique to the carbon monoxide flow considered here, the results presented in Fig. 4 can be shown to be qualitatively reasonable.

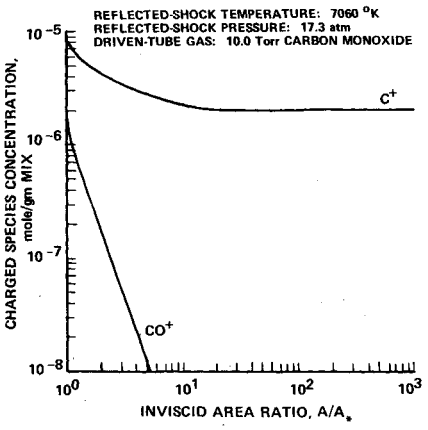

a)

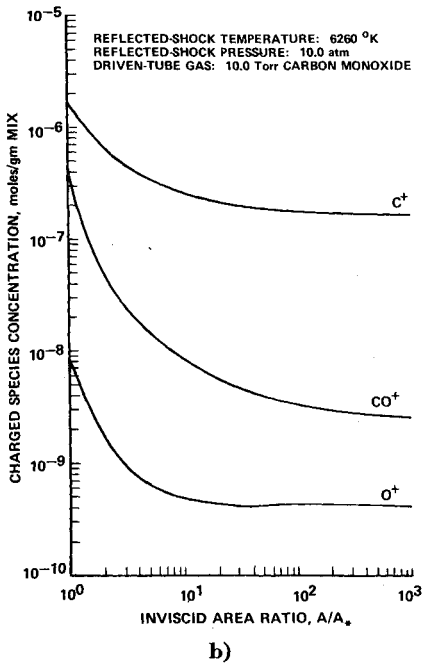

b)

Fig. 2 Ion-species distribution in nozzle flow.

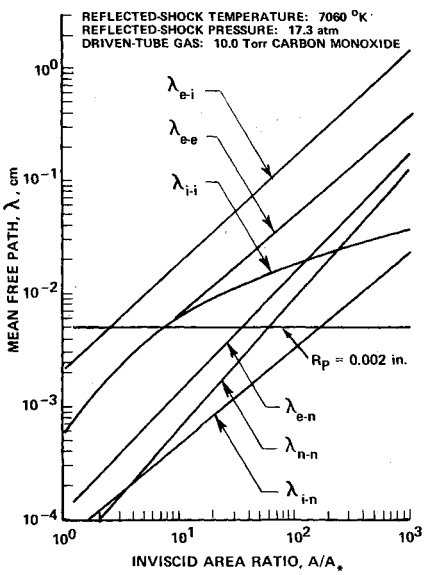

Fig. 3 Calculated mean free paths in carbon monoxide plasma.

The electron temperature appears to decrease slightly with increasing expansion ratios. At the first three measuring stations, the electron temperatures are seen to scatter approximately ±10% about an average value. At the last measuring station the scatter is somewhat greater. The dashed line faired through the measurements represents the electron temperature used in the rate-coefficient determination.

The electron-density measurements performed in the expansion are shown on Fig. 5. The measurements are seen to scatter by approximately ±15% about an average value. Much of this scatter can be correlated with the run-to-run variation in the shock-tube incident-shock velocity.

It was previously noted that for these experiments the neutral-chemistry reactions were relatively unimportant. All of the charged-chemistry reactions given in Table 1 were included in the calculations but the only one of importance was reaction 13. In correlating the experimental data we have adopted the $T_e^{-4.5}$ temperature dependence[5,6] for this reaction and the $T_e^{-1.5}$ temperature dependence[1-3] for reaction 12. We do not feel that our results are sufficiently sensitive to temperature dependence to merit any change from these predicted temperature variations.

In order to demonstrate the dominance of reaction 13, the rate coefficient for each of the reactions 12, 7, 9, and 10 was individually decreased or increased by a factor of 10 and the nonequilibrium calculation repeated. For none of these rate-coefficient perturbations did the predicted electron density change by more than 15%. It can therefore be concluded that the rate coefficients for these reactions given in Table 1 can be considerably in error without affecting the rate coefficient obtained from these experiments for the reaction $C^+ + e^- + e^- \rightarrow C + e^-$. By contrast, the influence of the rate coefficient for reaction 13 on the predicted electron-density distribution is shown on Fig. 5. Line A on this figure represents the predicted result using the theoretical rate coefficient of Ref. 4 and is seen to slightly over-predict the measured results. By increasing their predicted rate coefficient by a factor of 3.5 (line D) or less (lines B and C) all of the experimental data can be correlated. A rate coefficient of $(6.0 \pm 2) \times 10^{-8} T_e^{-4.5}$ correlates the experimental data reasonably well.

Line E on Fig. 5 illustrates that the electron temperature has an important influence on the predicted electron-density distribution for this reservoir condition. This result was ob-

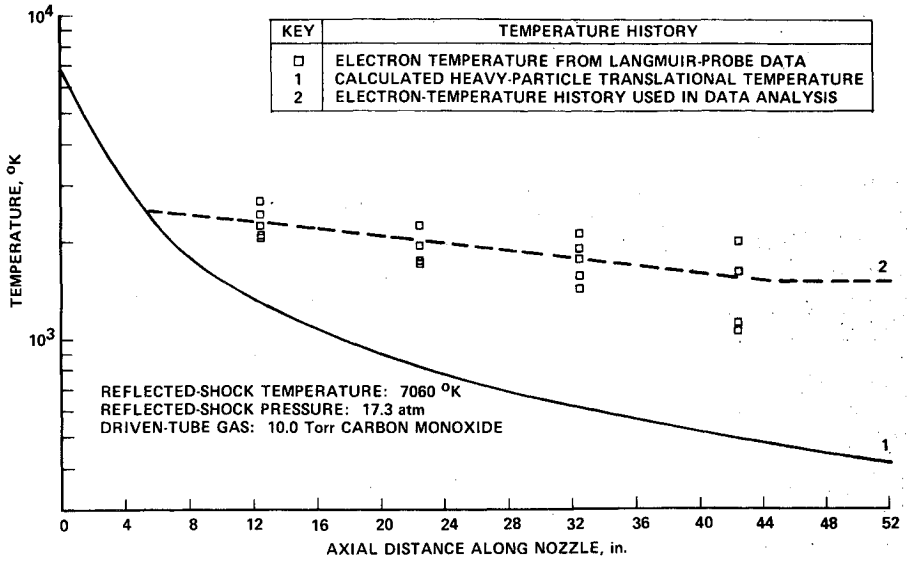

Fig. 4 Measured electron temperature in expanding carbon monoxide plasma.

tained using the same rate coefficients as used for line D but the heavy-particle translational temperature was used instead of the electron temperature in the rate-coefficient expression. The effect of the temperature history is seen to be a reduction in the predicted electron density at $A/A* = 1000$ of about 1.6. At smaller area ratios, the importance of the temperature history can be seen to be reduced.

Figure 6 presents a comparison between the data of this paper and previous reaction rate-coefficient data and predictions for the class of reactions given by $M^+ + e^- + e^- \rightarrow M + e^-$. To the author's knowledge, there are no other data for the $C^+ + e^- + e^- \rightarrow C + e^-$ reaction with which the present results could be compared. As can be seen from Fig. 6 the predictions of Makin and Keck[5] and Mansbach and Keck,[6] bound reasonably well the available data for hydrogen, helium, and nitrogen. The results of Ref. 5 overpredict these data by about the same amount as the results of Ref. 6 underpredict the data. On the basis of this comparison with experimental results, both theories appear to represent the data reasonably well. However, since they are independent of the ion undergoing recombination, they might be expected to also correlate the remaining data presented on Fig. 6. As illustrated, the Mansbach-Keck prediction falls below almost all of the experimental data while the Makin-Keck prediction falls above the hydrogen-helium-nitrogen data and below the mercury-argon-cesium and carbon data. Also included on Fig. 6 is the theoretical prediction of recombination rate for atomic nitrogen suggested by Park[17] which is in good agreement with that of Makin and Keck. The carbon data presented here are about a factor of three greater than these later predictions in the mid-temperature range. In view of the three predictions presented on Fig. 6 and also taking into consideration the mercury-argon-cesium data, the agreement between the data presented here and

REFLECTED-SHOCK TEMPERATURE: 7060 °K
REFLECTED-SHOCK PRESSURE: 17.3 atm
DRIVEN-TUBE GAS: 10.0 Torr CARBON MONOXIDE

KEY	REACTION RATE COEFFICIENT FOR $C^+ + e^- + e^- \rightarrow C + e^-$	TEMPERATURE HISTORY FROM FIGURE 4
A	$2.31 \times 10^{-8} T_e^{-4.5}$	2
B	$5.22 \times 10^{-8} T_e^{-4.5}$	2
C	$6.20 \times 10^{-8} T_e^{-4.5}$	2
D	$8.10 \times 10^{-8} T_e^{-4.5}$	2
E	$8.10 \times 10^{-8} T^{-4.5}$	1

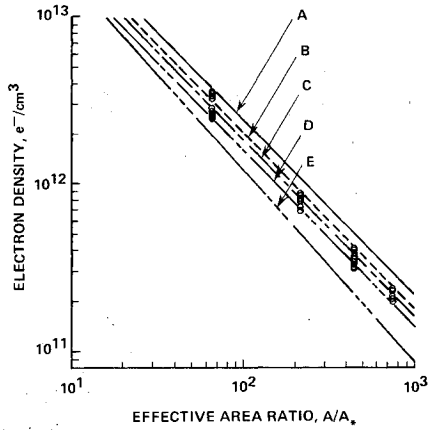

Fig. 5 Electron-density distribution in expanding carbon monoxide plasma.

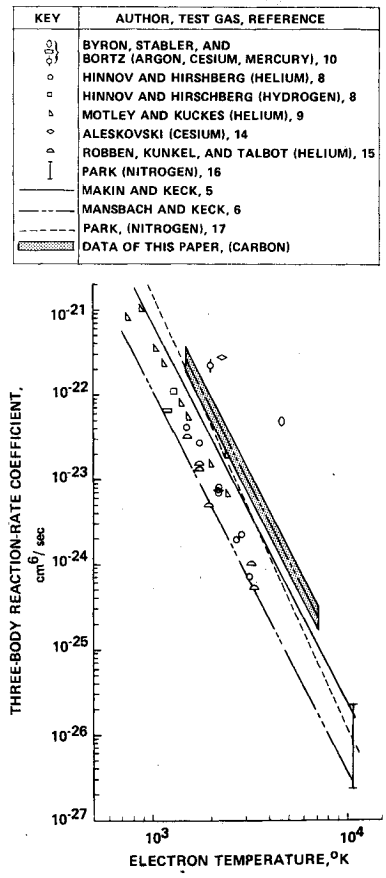

Fig. 6 Reaction-rate-coefficient data and theory for the reaction $M^+ + e^- + e^- M \rightarrow + e^-$.

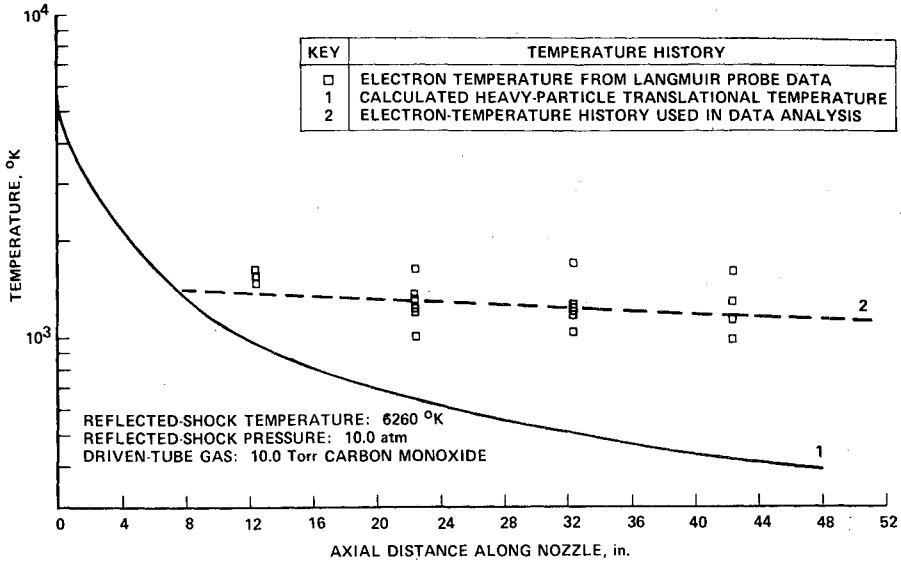

Fig. 7 Measured electron temperature in expanding carbon monoxide plasma.

the predictions of Makin and Keck and Park is reasonably good.

$CO^+ + e^- \rightarrow C + O$ Reaction

Microwave-interferometer and Langmuir-probe measurements were also performed at the same axial locations as previously described for a reservoir condition of 6260°K at 10.0 atm pressure. The boundary-layer growth for this condition was somewhat different than calculated for the previous condition which accounts for why the results are plotted at different area ratios for the same axial location.

The measured electron-temperature distribution in the expansion is presented in Fig. 7 along with the calculated heavy-particle translational temperature. The electron temperature is shown to decrease slightly in the region from 12.5 to 22.5 in. but to remain relatively uniform beyond 22.5 in. from the throat. The scatter in these measurements is somewhat larger than previously experienced but consistent with that obtained at 42.5 in. for the previous experimental condition (see Fig. 4). The dashed line faired through the data was used in determining the reaction rate coefficient.

The measured electron densities are presented in Fig. 8 as a function of inviscid area ratio. The scatter in these measurements is consistent with that experienced at the previous experimental condition. However, the results obtained at the last station appear to be high by about 15% based upon extrapolation of the three upstream results. The reason for this is not known but it is possibly due to an inaccuracy in the boundary-layer correction at this downstream location.

Again the neutral-species reactions were unimportant in the expansion. However, for this reservoir condition, reactions 7, 8, 9, 10 and 12 were dominant (all proceeding in the opposite direction to that written in Table 1) and of approximately equal importance. The three-body reactions 13 and 14 were relatively unimportant even though the dominant ion in the expansion was C^+ (Fig. 2b). The calculations have demonstrated that the reactions controlling the C^+ concentration level are the reactions 7–10 and 12.

The fact that the ion-molecule and ion-atom charge transfer reactions have a significant influence on the predicted electron-density distributions is unfortunate for the purposes of this study in light of the previously noted uncertainty in the associated reaction rate coefficients. At the present time it seems reasonable to accept the rate coefficients given in Table 1 for these reactions and proceed with the data reduction. It is, however, important to realize that the results may have to be modified if data for these reactions were to become available.

Lines A, B, and C on Fig. 8 illustrate the influence of the $CO^+ + e^-$ rate coefficient on the calculated electron-density distribution, accepting the rates given in Table 1 for reactions 7–11. The temperature dependence of this reaction was assumed to be $T_e^{-1.5}$ on the basis of previous work by Hansen,[28] O'Malley,[29] Cunningham and Hobson.[30] The calculations were performed using the measured electron-temperature distribution. With the exception of the most downstream data, the electron-density measurements are well correlated by a rate coefficient given by $k_{r_2} = (2.5 \pm 0.5) \times 10^{-2} T_e^{-1.5}$. The influence of using the electron temperature instead of the heavy-particle translational temperature in performing the calculations is insignificant as can be seen by comparing lines C and D.

Comparison of line E with line C shows the influence of the ion-atom rate coefficient on the predicted electron-density distribution. For this particular calculation, the rate of reaction 9 was decreased by a factor of 5 resulting in a decrease in the electron density of approximately a factor of 1.8. A corresponding decrease in the rates of reactions 8 and 10 pro-

REFLECTED-SHOCK TEMPERATURE: 6260 °K
REFLECTED-SHOCK PRESSURE: 10 atm
DRIVER-TUBE GAS: 10 Torr CARBON MONOXIDE

KEY	REACTION RATE COEFFICIENT FOR $CO^+ + e^- \rightarrow C + O$	TEMPERATURE HISTORY FROM FIGURE 7
A	$1.11 \times 10^{-2} T_e^{-1.5}$	2
B	$1.99 \times 10^{-2} T_e^{-1.5}$	2
C	$2.82 \times 10^{-2} T_e^{-1.5}$	2
D	$2.82 \times 10^{-2} T^{-1.5}$	1
E	$2.82 \times 10^{-2} T_e^{-1.5}$	2

NOTE: FOR CALCULATION "E", THE RATE COEFFICIENT FOR THE REACTION $C + O^+ \rightarrow C^+ + O$ HAS BEEN DECREASED BY A FACTOR OF 5.

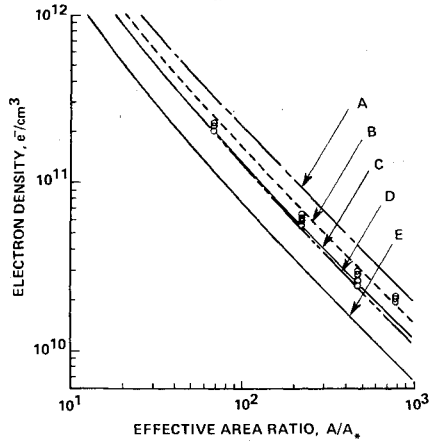

Fig. 8 Electron density distribution in expanding carbon monoxide plasma.

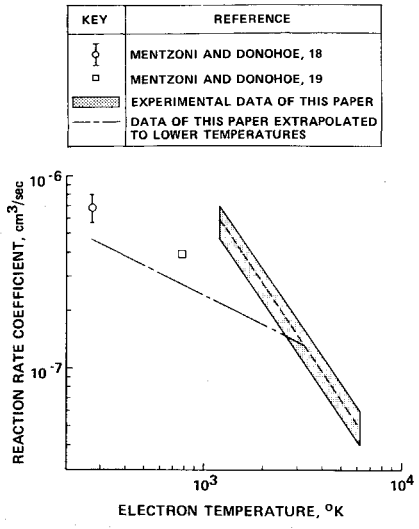

Fig. 9 Reaction rate coefficient data for the reaction $CO^+ + e^- \rightarrow C + O$.

duces a similar result. However, a decrease of a factor of 5 in the rate coefficient for reaction 7 results in an increase in predicted electron density by a factor of approximately 1.8. These calculations illustrate that the results presented here for the $CO^+ + e^-$ rate coefficient are sensitive to the rate coefficients of reactions 7–10.

The reaction rate-coefficient expression obtained here for the deionization of CO^+ at high temperatures is consistent with previous measurements[1–3] for the $NO^+[k_r = (1.1 \pm 0.4) \times 10^{-2}T_e^{-1.5}]$, $N_2^+[k_r = (2.5 \pm 0.8) \times 10^{-2}T_e^{-1.5}]$, and $O_2^+[k_r = (1.3 \pm 0.3) \times 10^{-2}T_e^{-1.5}]$ two-body dissociative recombination reactions. Though this comparison is only qualitative, it does suggest that the rate coefficients for the charge-transfer reactions are not drastically in error.

Figure 9 presents a comparison between the $CO^+ + e^-$ rate coefficient data of this paper and the previous low-temperature data of Mentzoni and Donohoe.[18,19] The measurements were not obtained at comparable electron temperatures so direct comparison is not possible. However, the present data can be extrapolated to lower temperatures by applying the technique used by Hansen[28] in his $NO^+ + e^-$ study and by ourselves in our $N_2^+ + e^-$ and $O_2^+ + e^-$ studies.[2,3] The procedure used here was to match a $T_e^{-0.5}$ temperature dependence to our data at the characteristic vibrational temperature of CO^+ ($\theta_v = 3140°K$). This extrapolation is seen to agree reasonably well with the low-temperature data of Mentzoni and Donohoe.

Conclusions

The $C^+ + e^- + e^-$ three-body recombination rate coefficient and the $CO^+ + e^-$ two-body dissociative recombination rate coefficient have been measured in carbon monoxide plasmas that have expanded from equilibrium reservoir conditions of 7060°K at 17.3 atm pressure and 6260°K at 10.0 atm pressure respectively. The resulting reaction rate coefficient for the recombination of C^+ is given by $k_{r_1} = (6.0 \pm 2) \times 10^{-8}T_e^{-4.5}$ cm^6/sec for an electron temperature range of approximately 1500°K–7000°K. The reaction rate coefficient for the recombination of CO^+ is given by $k_{r_2} = (2.5 \pm 0.5) \times 10^{-2}T_e^{-1.5}$ cm^3/sec for an electron temperature range of approximately 1200°–6200°K. The reader is cautioned that in order to obtain the CO^+ deionization rate coefficient it was necessary to estimate the rate coefficients for several of the charge-transfer reactions. However, the results obtained are consistent with the dissociative recombination rate coefficients obtained for NO^+, N_2^+ and O_2^+.

References

[1] Dunn, M. G. and Lordi, J. A., "Measurement of Electron Temperature and Number Density in Shock-Tunnel Flows: Part II, $NO^+ + e^-$ Dissociative Recombination Rate in Air," *AIAA Journal*, Vol. 7, No. 11, Nov. 1969, pp. 2099–2104.

[2] Dunn, M. G. and Lordi, J. A., "Measurement of $N_2^+ + e^-$ Dissociative Recombination in Expanding Nitrogen Flows," *AIAA Journal*, Vol. 8, No. 2, Feb. 1970, pp. 339–345.

[3] Dunn, M. G. and Lordi, J. A., "Measurement of $O_2^+ + e^-$ Dissociative Recombination in Expanding Oxygen Flows," *AIAA Journal*, Vol. 8, No. 4, April 1970, pp. 614–618.

[4] Curry, B. P., "Collisional Radiative Recombination in Hydrogen Plasmas and in Alkali Plasmas," *Physical Review A*, Vol. 1, No. 1, Jan. 1970, pp. 166–176.

[5] Makin, B. and Keck, J. C., "Variational Theory of Three-Body Electron-Ion Recombination Rates," *Physical Review Letters*, Vol. 11, No. 6, Sept. 1963, pp. 281–283.

[6] Mansbach, P. and Keck, J., "Monte Carlo Trajectory Calculations of Atomic Excitation and Ionization by Thermal Electrons," *Physical Review*, Vol. 181, No. 1, May 1969, pp. 275–289.

[7] D'Angelo, N., "Ion-Electron Recombination," *Physical Review*, Vol. 140, No. 5A, Nov. 1965, p. A1488.

[8] Hinnov, E. and Hirschberg, J. G., "Electron-Ion Recombination in Dense Plasmas," *Physical Review*, Vol. 125, No. 3, Feb. 1962, pp. 795–801.

[9] Motley, R. W. and Kuckes, A. F., "Recombination in a Helium Plasma," *Proceedings of the Fifth International Conference on Ionic Phenomena*, Munich, 1961, North-Holland Publishing Co., Amsterdam, 1964, pp. 651–659.

[10] Byron, S., Stabler, R. C., and Bortz, P. I., "Electron-Ion Recombination by Collisional and Radiative Processes," *Physical Review Letters*, Vol. 8, No. 9, May 1962.

[11] Dugan, J. W., "Three-Body Collisional Recombination of Cesium Seed Ions and Electrons in High Density Plasmas with Argon Carrier Gas," TN D-2004, Oct. 1964, NASA.

[12] Abramov, V. A., "Electron-Ion Recombination in a Cesium Plasma," *Teplo fizika Vysokikh Temperatur*, Vol. 3, No. 1, Jan.-Feb. 1964, pp. 23–27.

[13] D'Angelo, N., "Recombination of Ions and Electrons," *Physical Review*, Vol. 121, No. 2, Jan. 1961, pp. 505–507.

[14] Aleskovski, Y. M., "Investigation of Volume Recombination in a Cesium Plasma," *Soviet Physics JETP*, Vol. 17, No. 3, Sept. 1963, pp. 570–575.

[15] Robben, F., Kunkel, W. B., and Talbot, L., "Spectroscopic Study of Electron Recombination with Monatomic Ions in a Helium Plasma," *Physical Review*, Vol. 132, No. 6, Dec. 1963, pp. 2363–2371.

[16] Park, C., "Measurement of Ionic Recombination Rate of Nitrogen," *AIAA Journal*, Vol. 6, No. 11, Nov. 1968, pp. 2090–2094.

[17] Park, C., "Collisional Ionization and Recombination Rates of Atomic Nitrogen," *AIAA Journal*, Vol. 7, No. 8, Sept. 1969, pp. 1653–1654.

[18] Mentzoni, M. H. and Donohoe, J., "Electron Removal During the d.c. Discharge Afterglow of Carbon Monoxide," *Physics Letters*, Vol. 26A, No. 7, Feb. 1968, pp. 330–331.

[19] Mentzoni, M. H. and Donohoe, J., "Electron Recombination and Diffusion in CO at Elevated Temperatures," *Canadian Journal of Physics*, Vol. 47, 1969, pp. 1789–1795.

[20] Lordi, J. A., Mates, R. E., and Moselle, J. R., "Computer Program for the Numerical Solution of Nonequilibrium Expansions of Reacting Gas Mixtures," AD-1689-A-6, June 1965, Cornell Aeronautical Lab., Buffalo, N. Y.

[21] Fehsenfeld, F. C., Schmeltekopf, A. L., and Ferguson, E. E., "Thermal-Energy Ion-Neutral Reaction Rates vs Measured Rate Constants for C^+ and CO^+ Reactions with O_2 and CO_2," *The Journal of Chemical Physics*, Vol. 45, No. 1, July 1966, pp. 23–25.

[22] Burke, A. F. and Wallace, J. E., "Aerothermodynamic Consequences of Nozzle Nonequilibrium," TR-66-45, Feb. 1966, Arnold Engineering Development Center, Tullahoma, Tenn.

[23] Laframboise, J. G., "Theory of Cylindrical and Spherical Langmuir Probes in a Collisionless, Maxwellian Plasma at Rest," *Rarefied Gas Dynamics*, Vol. II, Academic Press, New York, 1965, pp. 22–44.

[24] Talbot, L. and Chou, Y. S., "Langmuir Probe Response in the Transition Regime," *Proceedings of the Sixth Rarefied Gasdynamics Symposium*, Vol. II, Office of Naval Research, Office of Scientific Research, NASA, June 1968, pp. 1723–1738.

[25] Sonin, A. A., "The Behavior of Free Molecule Cylindrical Langmuir Probes in Supersonic Flows, and Their Application to the Study of the Blunt Body Stagnation Layer," Rept. 109, Aug. 1965, Univ. of Toronto Inst. for Aerospace Studies, Toronto, Canada.

[26] Dunn, M. G. and Lordi, J. A., "Thin-Wire Langmuir-Probe Measurements in the Transition and Free-Molecular Flow Regimes," *AIAA Journal*, Vol. 8, No. 6, June 1970, pp. 1077–1081.

[27] Lordi, J. A. and Dunn, M. G., "Sources of Electron Energy in Weakly Ionized Expansions of Nitrogen," AI-2187-A-16, Aug. 1969, Cornell Aeronautical Lab., Inc., Buffalo, N. Y.

[28] Hansen, C. F., "Temperature Dependence of the $NO^+ + e^-$ Dissociative Recombination-Rate Coefficient," *The Physics of Fluids*, Vol. 11, No. 4, April 1968, pp. 904–906.

[29] O'Malley, T. F., "On the Temperature Dependence of the Dissociative Recombination Rate," *6th Electronic and Atomic Collisions Conference*, 1969, Boston, Mass., see also *Physical Review*, Vol. 185, No. 1, Sept. 1969, pp. 101–104.

[30] Cunningham, A. J. and Hobson, R. M., "Experimental Measurements of Dissociative Recombination in Vibrationally Excited Gases," *Physical Review*, Vol. 185, No. 1, 1969, pp. 98–100.

NOVEMBER 1971 AIAA JOURNAL VOL. 9, NO. 11

A Study of Hollow Cathode Discharge Characteristics

C. M. PHILIP*
Royal Aircraft Establishment, Farnborough, Hampshire, England

The operation and performance of small-orifice hollow cathodes for use in electron bombardment ion thrusters is described. Using mercury propellant, vaporized either in a small boiler or by a heated porous plug, cathodes have been operated in both a simple test facility and in an ion thruster. Voltage-current characteristics were obtained by a novel rapid-scan technique, and the dependence of these on parameters such as vapor flow rate and temperature has been studied. An examination of such characteristics has enabled a qualitative theory of the cathode discharge to be proposed, which is consistent with the observed behavior. Cathodes have been operated for periods exceeding 1000 hr without any apparent deterioration of performance.

Introduction

THE majority of electron bombardment ion thrusters using mercury propellant employ hollow cathodes[1] for both the main discharge and neutralizer.[2] In order to make the most efficient use of such cathodes in these applications, it is necessary to obtain extensive information concerning the dependence of their characteristics on parameters such as vapor flow rate, temperature, and constructional dimensions. It was the aim of the work described here to develop a suitable cathode, to obtain this information both in a simple test facility and in an operating thruster, and to optimize the design to achieve high efficiency and long operational life.

At the present time, a successful cathode design has been evolved, and preliminary life tests have shown that orifice erosion can probably be overcome. Using mercury vapor from either a small boiler or a porous plug vaporizer, cathodes have been operated under widely varying conditions in both a laboratory vacuum chamber and in an ion thruster test facility.

Voltage-current characteristics have been obtained using a new technique and indicate that suitable operating points exist for both main discharge and neutralizer applications. In addition, it was possible, using the information gained, to propose a discharge mechanism, including appropriate electron emission processes, which was qualitatively consistent with experiment.

Presented as Paper 70-1087 at the AIAA 8th Electric Propulsion Conference, Stanford, Calif., August 31–September 2, 1970; submitted October 21, 1970; revision received May 7, 1971. British Crown Copyright reproduced with the permission of the Controller, Her Britannic Majesty's Stationery Office. The author wishes to thank D. G. Fearn for helpful advice throughout the course of this work. Thanks are also due to A. A. Wells of Culham Laboratory and G. L. Davis and M. G. Charlton of Mullard Ltd. for many fruitful discussions.

Index category: Electric and Advanced Space Propulsion.

* Scientific Officer, Space Department.

Cathode Construction

The types of hollow cathode used were similar in configuration to the neutralizer cathode described by Rawlin and Pawlik,[2] the basic design features being illustrated in Fig. 1. The cathode tip was a tungsten disk (1 mm thick and 3.5 mm diam) electron-beam welded into a tantalum tube. It was provided with a central orifice of between 100 and 350 μm diam formed by either spark erosion or diamond drilling. A stainless-steel flange at the upstream end of the cathode was provided for mating with other components.

Cathode Heater

Two methods were used for encapsulating the cathode heater, which was made from 15 turns of 200-μm-diam tungsten-3% rhenium wire, electro-polished before winding. One method employed alumina particles flame-sprayed onto the cathode body. In this case, a thin intermediate layer of molybdenum was applied to the tantalum tube to provide a bond for the alumina and to prevent an alumina-tantalum reaction at elevated temperatures. In the second method, a zirconia-based ceramic adhesive was applied in paste form and was subsequently hardened and cured.

Emitting Surface

To produce an electron-emitting coating, a layer of triple carbonate mixture was applied to the internal surface of the tantalum tube. The carbonates were reduced on raising the temperature to about 1200°K in vacuo, and a low work function surface of chiefly barium oxide was formed.

Apparatus

Most of the experiments were performed in a glass chamber evacuated by a mercury diffusion pump. The pressure was monitored by means of Pirani and ionization gages. The hollow cathodes were bolted, either directly or via an inter-